



**STScI** | SPACE TELESCOPE  
SCIENCE INSTITUTE

Instrument Science Report COS 2023-07(v1)

# COS FUV Detector Gain Maps Obtained at the Start of LP6 Operations

---

Christian I. Johnson<sup>1</sup> and David Sahnou<sup>1</sup>

<sup>1</sup>Space Telescope Science Institute, Baltimore, MD

15 April 2023

---

## ABSTRACT

*A sixth lifetime position (LP6) was enabled on the Cosmic Origins Spectrograph (COS) in October 2022 in an effort to maximize the lifetime and scientific output of the far-ultraviolet (FUV) detector. We present the results of Visit 5C for Program 16829, which used the on-board Deuterium lamps to illuminate the LP6 region of the COS FUV detector with the goal of measuring the modal gain for the start of LP6 operations. The resulting gain maps indicate that the starting high voltage values are appropriate for both the FUV A (167) and FUV B (169) segments. No gain sag holes are found on the FUV A segment, but the FUV B segment has several sagged columns in regions that overlap with LP5 G130M/1291 Lyman  $\alpha$ . These holes were expected due to the close proximity of LP5 and LP6 on the detector, and the majority of the pixels in the LP6 rows have modal gain larger than 6.*

---

## Contents

1. Introduction . . . . .	2
2. Observations . . . . .	3
3. Analysis and Results . . . . .	4
Change History for COS ISR 2023-07 . . . . .	6
References . . . . .	6

## 1. Introduction

The COS FUV cross-delay-line (CDL) detector is a photon-counting microchannel plate device capable of observing wavelengths between approximately 900 Å and 2150 Å. Photon events are recorded when an incident UV photon strikes the detector and creates a cascade of electrons. The detector electronics register the two-dimensional location and total charge (pulse height) of each event, and over the course of an exposure all events falling within a digitized pixel can be summed to create a pulse height distribution (histogram). The pulse height distribution is then fit with an analytic function and the peak location recorded as the “modal gain”. The modal gain traces the number of electrons generated for every detected photon event, and is used to measure the microchannel plate’s local response and sensitivity.

Long-term exposure to light decreases the efficiency of the photon-to-electron conversion in the COS FUV detector, which manifests as a decrease in the modal gain value of a pixel with time. When the modal gain of a pixel reaches a value of 3, approximately 5% of incident source photons fail to produce a pulse height high enough to be recorded and the pixel is considered “sagged” (Sahnou et al. 2011). Permanently sagged pixels therefore suppress the number of observed counts from a target and cause gain sag holes to appear in the extracted science spectra. Gain sag holes can form rapidly in detector regions that accumulate high count levels, such as where geocoronal Lyman  $\alpha$  falls. Gain sag can be mitigated by increasing the high voltage on the desired segment, which shifts the pulse height distribution to higher values, or by projecting the spectra to a different place on the detector (lifetime position; LP) where the modal gain is higher.

Prior to the start of LP4 operations (October 2, 2017), the HV on a given segment was increased as soon as a gain sag hole formed, and when a hole formed at the highest allowed HV setting on either segment all exposures were moved to a new LP. Starting with LP4, a new set of “COS2025” rules was enabled in an effort to extend the lifetime

of COS through at least 2025 (Oliviera et al. 2018). The COS2025 rules permitted Lyman  $\alpha$  gain sag holes from G130M/1291 to form without triggering a HV increase or LP change. Starting with LP5 (October 4, 2021), COS enabled a “hybrid mode” operation where different configurations utilized different LP and/or HV settings. In the Cycle 29 setup, G130M/1055 and 1096 (“blue modes”) are observed at LP2, G140L modes are observed at LP3, G130M/1222 and G160M modes operate at LP4, and G130M/1291, 1300, 1309, 1318, and 1327 modes are observed at LP5. This was expanded with the activation of LP6 (Cycle 30) that moved most G160M observations from LP4 to LP6.

As with all previous new LPs, when a new LP is enabled a series of internal deuterium lamp exposures is taken within the first 1-2 weeks of operation in order to both verify that the modal gain values of all pixels, omitting those that may be sagged near G130M/1291, are still  $> 3$  and to have baseline gain maps for future detector modeling and monitoring. As noted in Sahnou (2019) these standard gain map programs are taken using both the G130M/1309 and G160M/1600 settings in order to maximize coverage on both segments while minimizing exposure times. The exposures from both cenwaves are then combined in order to generate robust pulse height distributions for all pixels of interest. For previous LPs, an LP-specific calibration program was designed and executed in order to create the initial gain maps. However, since LP5 and LP6 have several overlapping rows and currently operate at the same HV (167 for FUV A and 169 for FUV B), the initial LP6 gain maps can be generated from the standard gain map monitoring program that executes every 6 months, which includes the start of LP6.

## 2. Observations

The LP6 gain map data were acquired as part of Program 16829 (P. I. Sahnou), which takes Deuterium lamp exposures of all active lifetime positions at the beginning and mid-point of each cycle. Since the LP5 gain map data are acquired with the Flat-Field Calibration Aperture (FCA) mechanism near the soft-stop limit, we are unable to project Deuterium lamp exposures higher on the detector for LP6. However, Figure 1 shows that the LP5 gain map FCA position is sufficient to project the Deuterium lamp high enough to cover nearly all LP6 rows of both segments with a sufficient number of counts (25 counts per  $2 \times 8$  binned super-pixel) to measure the modal gain. Therefore, we utilized data from Visit 5C of Program 16829 to create the LP6 gain maps.

Visit 5C utilized the gain map procedure outlined in Section 2 of Johnson & Sahnou (2021), which initializes the setup with a 125 second LP1 Deuterium lamp exposure, adjusts the HV to the appropriate level (167/169 for FUV A/FUV B), and then executes a series of aperture movements and exposures with the G130M/1309 and G160M/1600 cenwaves before returning the aperture to the home position. Details of this procedure

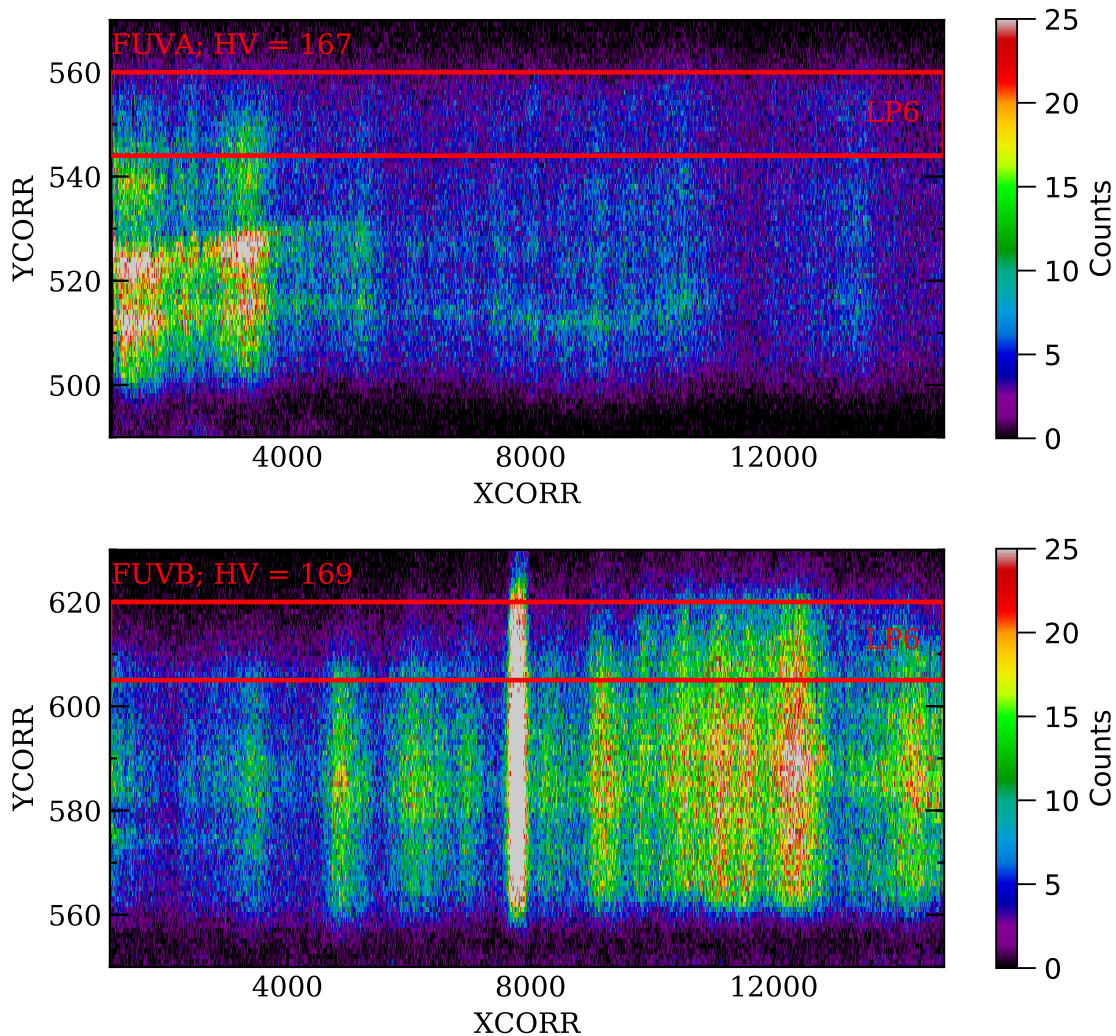


**Figure 1.** The top (FUVA) and bottom (FUVB) panels show summed count maps for all LP6 gain map exposures taken for Program 16829. The red boxes show the approximate locations where LP6 G130M/1533, 1577, 1589, 1600, 1611, and 1623 will project. The bright, extended feature near the center of FUVB is Lyman  $\alpha$  from the deuterium lamp. The data are shown with  $1 \times 1$  (spatial  $\times$  dispersion) binning.

for Visit 5C of Program 16829 are shown in Table 1.

### 3. Analysis and Results

Modal gain values were extracted from the count maps shown in Figure 1 by binning the data  $2 \times 8$  (cross-dispersion  $\times$  dispersion), which creates square super-pixels and increases the number of counts per measurement, and then fitting an analytic function to the resulting pulse height distributions. Since the pulse height distributions are rarely

symmetric and often have long tails, we fit each super-pixel pulse height distribution with a skewed Gaussian profile of the form:

$$f(p_h) = \frac{A}{\sigma\sqrt{2\pi}} e^{-\frac{(p_h-\mu)}{2\sigma^2}} \left\{ 1 + \operatorname{erf} \left[ \frac{\gamma(p_h - \mu)}{\sigma\sqrt{2}} \right] \right\}, \quad (1)$$

where  $A$  is the fit amplitude,  $p_h$  is the observed pulse height bin,  $\mu$  is the fit centroid of the Gaussian component,  $\sigma$  is the dispersion of the Gaussian component,  $\gamma$  is the skewness factor, and  $\operatorname{erf}$  is the error function<sup>1</sup>. A sample pulse height distribution fit is shown in Figure 2. For each fit super-pixel, the modal gain is recorded as the global maximum (“peak”) of the fit. Note that fits for which the  $R^2$  residual metric are  $< 0.90$  are not recorded in the final gain maps.

Figure 3 shows the derived gain maps, expanded back to  $1 \times 1$  binning, for the FUV A and FUV B segments. The lower and upper bounds where G160M projects at LP6 are indicated by the black lines, which show that the LP5 gain maps produce enough counts to cover nearly all of FUV A and a majority of FUV B. The missing gain map information for  $\text{XCORR} < 6000$  and  $\text{YCORR} > 615$  does not cover regions where we expect low modal gain, and these regions are routinely monitored for gain sag with a separate procedure that uses weekly count maps of GO and calibration observations.

Figure 4 shows the lowest modal gain pixel for each column in the projected LP6 region of Figure 3. The top panel gain trace indicates that no gain sag is present in the FUV A segment at the start of LP6 operations. However, several columns in the LP6 region are sagged on FUV B, which is due to Lyman  $\alpha$  observations from G130M/1291 at LP5. This was expected for the start of LP6 operations because LP5 and LP6 are close on the detector and the COS2025 rules permit Lyman  $\alpha$  gain sag holes from forming before

<sup>1</sup>See [https://lmfit.github.io/lmfit-py/builtin\\_models.html](https://lmfit.github.io/lmfit-py/builtin_models.html) for more information about the fitting function.

**Table 1.** LP6 Gain Map Procedure (Visit 5C of Program 16829)

Root Name	Mode	LP	FP-POS	HV (A/B)	Exp. (s)	XAPER	XSTEPS	Notes
leqy5camq	TIME-TAG	1	1	178/175	125	N/A	N/A	LP1 Exp.
N/A	DATA	N/A	N/A	167/169	39	N/A	N/A	Adjust HV
N/A	ALIGN/APER	N/A	N/A	167/169	0	-60	N/A	Adjust aperture
leqy5cb0q	TIME-TAG	1	1	167/169	440	N/A	N/A	G130M/1309
N/A	ALIGN/APER	N/A	N/A	167/169	0	-114	-54	Adjust aperture
leqy5cb4q	TIME-TAG	1	1	167/169	440	N/A	N/A	G130M/1309
N/A	ALIGN/APER	N/A	N/A	167/169	0	-72	42	Adjust aperture
leqy5cb6q	TIME-TAG	1	4	167/169	440	N/A	N/A	G160M/1600
leqy5cbaq	TIME-TAG	1	4	167/169	440	N/A	N/A	G160M/1600
N/A	ALIGN/APER	N/A	N/A	167/169	0	387	501	Return aperture

The XSTEPS parameter is in the Qesiparms section of the Engineering Requirements in APT.

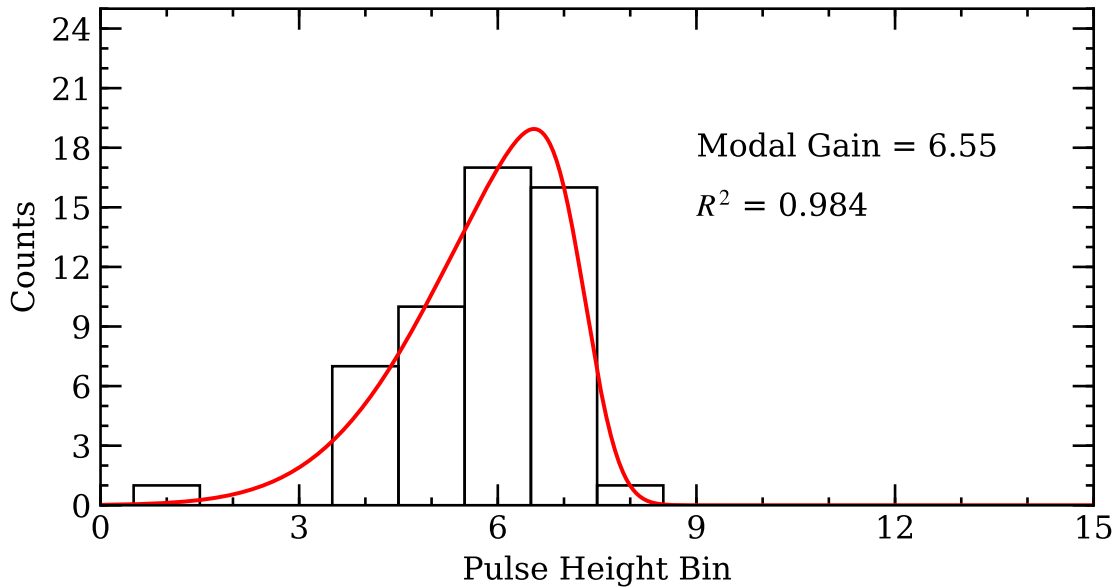


**Figure 2.** A sample pulse height distribution from a  $2 \times 8$  (spatial  $\times$  dispersion) super-pixel on the FUVB detector. The solid red line illustrates the best-fit skewed Gaussian profile of the pulse height distribution. The modal gain (global maximum of the fit) and  $R^2$  values are provided.

raising the HV. The “continuum” of LP6 on FUVB has modal gain values  $> 6$  for nearly all other pixels.

In summary, we show that the standard gain map program used for LP2 and LP5 reaches high enough on the detector to sufficiently measure the modal gain at LP6. Additionally, we demonstrate that the FUV pulse height distributions are better fit by skewed Gaussian profiles than pure normal distributions, as the former can account for the asymmetric wings. The results of this new fitting procedure indicate that the starting high voltage values for the FUVA (167) and FUVB (169) segments at LP6 are appropriate, and that the only gain sag holes present for the start of LP6 are those due to LP5 G130M/1291 observations.

## Change History for COS ISR 2023-07

Version 1: 15 April 2023- Original Document

## References

- Johnson, C. I., & Sahnou, D., 2021, COS Instrument Science Report 2021-12  
 Oliveira, C., De Rosa, G., Mackenty, J., et al., 2018, COS Instrument Science Report 2018-16

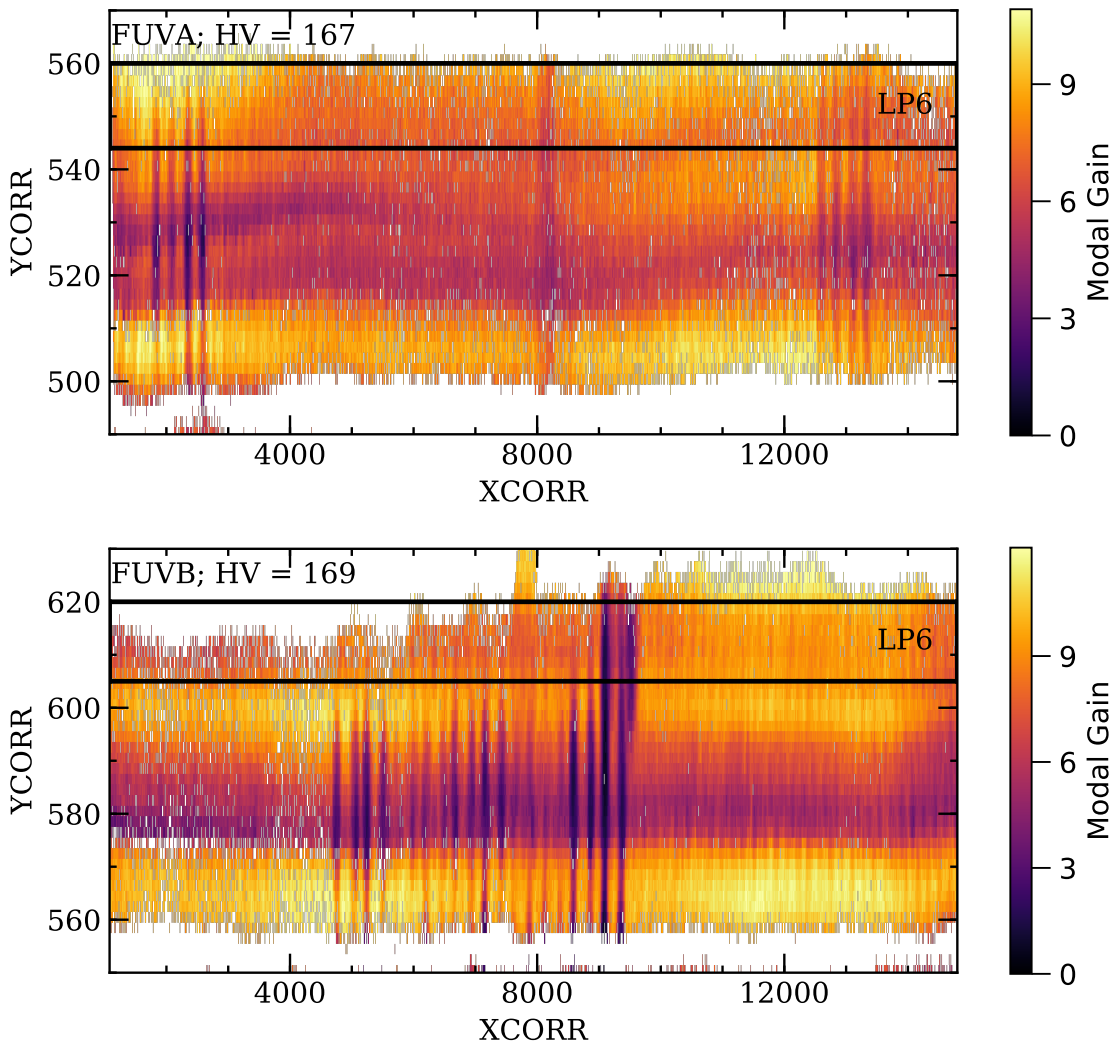


**Figure 3.** A 2D gain map constructed from the count map shown in Figure 1 and fitting procedure outlined in Figure 2 is illustrated along with the approximate projection of LP6 G160M data (black boxes). The FUVA segment is shown in the top row and the FUVB segment in the bottom row. The small gaps with no measurements represent pixels for which either not enough counts (25) are present or the  $R^2$  value from the fit are  $< 0.90$ . For FUVA, low gain regions on the left and right sides are due to previous Lyman  $\alpha$  observations at LP2 while the center feature is a known detector artifact. For FUVB, gain sag from G130M/1291 observations at LP5 affects some LP6 columns and rows. Although the FUVB deuterium lamp exposures do not cover the full LP6 projection, we do not expect rows 615-620 to have lower modal gain than rows 605-610.

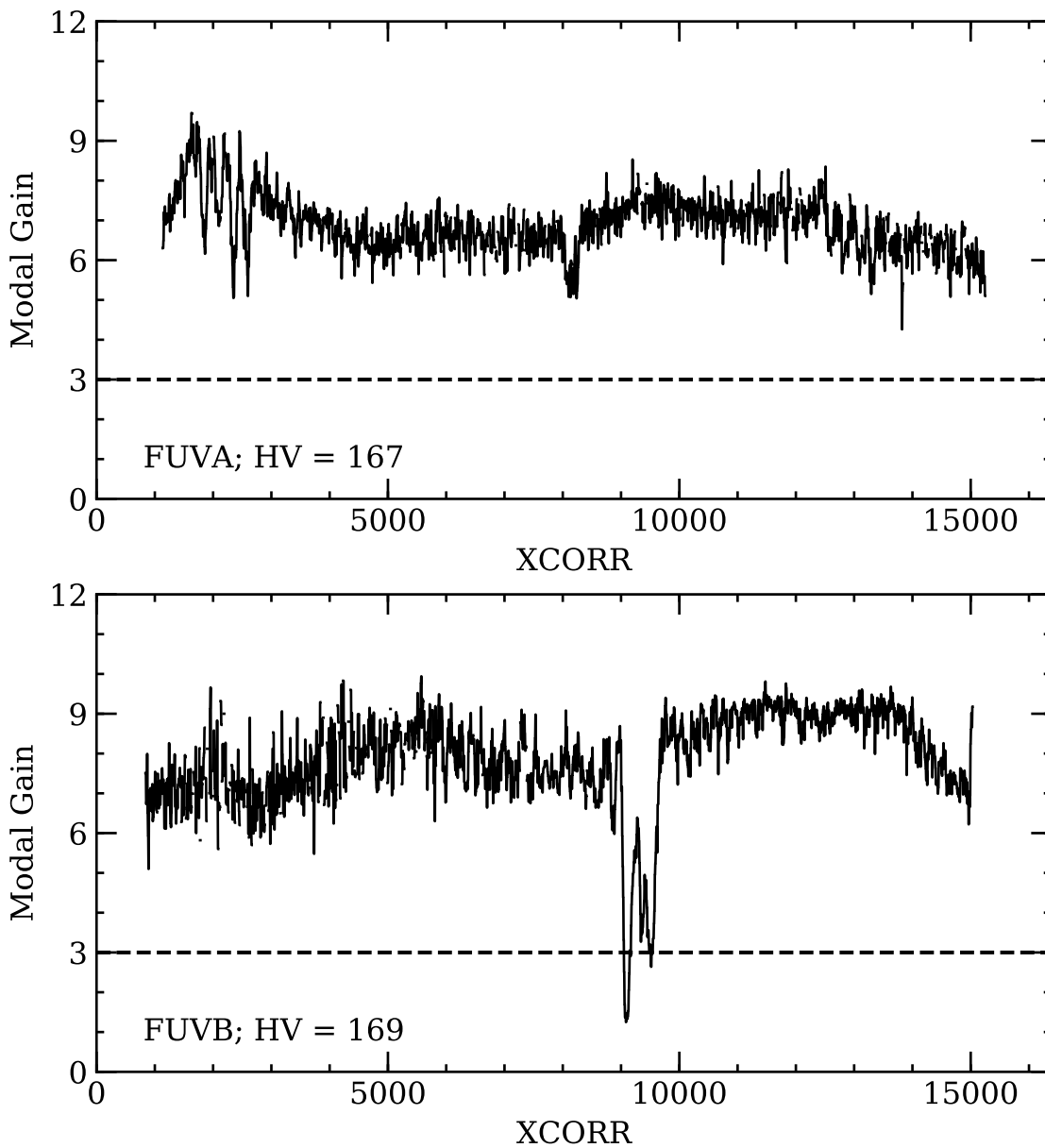


**Figure 4.** FUVA (top) and FUVB (bottom) gain traces at LP6 illustrate the lowest modal gain row for each column in the projection shown in Figure 3. A modal gain value of 3, which indicates pixel sag, is shown as a dashed black line in each panel. Note that the gain sag in the FUVB panel is accounted for in CalCOS by using the most up-to-date GSAGTAB reference file. The lower gain regions on FUVA near XCORR  $\sim$  2500 are due to previous LP2 usage while the low gain region near XCORR  $\sim$  8000 is from a detector artifact.

Sahnow, D., 2019, COS Instrument Science Report 2019-22  
Sahnow, D. J., Oliveira, C., Aloisi, A., et al., 2011, Proc. SPIE, 8145, 81450Q